

Direct FEM Ampacity Calculations for Submarine and Underground Power Cables

K. Bitsi, A.I. Chrysochos, and D. Chatzipetros
Hellenic Cables, Athens, Greece.

Abstract

The use of power cables has been rapidly increasing during the last decades, both in land and subsea applications. To reduce the cable cost, design optimization is necessary. The current-carrying capacity of cables, namely the “ampacity”, is an important factor, if not the most important one, significantly affecting the cable design. To optimize the latter, accurate ampacity calculations are required. The international standards, such as IEC, are typically used for ampacity calculations. However, they often adopt simplifications which may not lead to the optimum design. Two-dimensional heat transfer models, developed with the finite-element method (FEM), are presented in this paper. By using COMSOL Multiphysics® software, the typical ampacity calculations are improved both in accuracy and efficiency terms. By comparing FEM and Standard results, interesting findings occur and are discussed.

Keywords: Ampacity, FEM, modeling, optimization, submarine cables, underground cables.

Introduction

High-voltage power cables are vital components of power transmission systems. Submarine cables are critical power carriers between offshore wind farms and onshore ac grids. Moreover, underground cables are generally preferred over overhead installations in land applications, owing to environmental, aesthetic and reliability reasons [1].

To ensure the safe and reliable operation of power cables, it is crucial to estimate their ampacity most accurately and efficiently. The cable ampacity is dictated by the maximum operating temperature that the insulation can withstand without getting downgraded. For cables insulated with cross-linked polyethylene (XLPE), the thermal limit is typically set to 90°C. In practical applications, power cable loss and ampacity calculations are commonly performed using the IEC 60287 standard. Specifically, IEC 60287-1-1 provides the necessary formulas for the determination of the conductor resistance, sheath, dielectric and armor losses in a three-phase cable circuit [2]. These formulas are utilized by the proposed thermal circuit model in [2], which enables the computation of the permissible cable ampacity, by estimating the thermal resistances of the non-metallic parts of the cable. This model renders the thermal problem one-dimensional, as it assumes radial heat dissipation within the cable. However, this assumption does not entirely hold, especially in the case of three-core (3C) separate lead (SL)-type submarine cables, where the close physical proximity of the three cable cores leads to the inevitable distortion of their temperature fields [3]. Furthermore, in finite-element method (FEM) models, the heat transfer

equations are solved for temperature, which occurs as an output. Therefore, it is not feasible for someone to directly calculate the cable ampacity in the existing FEM models and, consequently, repetitive runs, including many trials, are required for this purpose.

In this paper, a two-dimensional (2D) FEM thermal cable model is developed, using COMSOL Multiphysics®¹ [4]. The purpose of this model is to compute the ampacity of the investigated cable in a direct manner, given the predetermined upper thermal limit. While losses are imported according to the IEC 60287-1-1 standard, considering also the recommendations provided by CIGRE TB 880 [5], the use of the 2D FEM solver allows for the inclusion of heat proximity effects in the analysis [6]. To effectively determine the cable ampacity, two approaches are adopted: first, a direct ampacity method is employed, by pre-assuming the hottest cable core and assigning a Dirichlet condition on that; subsequently, a more generic method, making use of the Optimization Module of COMSOL Multiphysics®, is employed and used to validate the direct ampacity method. Both submarine and underground cable designs are investigated. The results of this study are compared with the corresponding thermal calculations obtained using the commercial software CYMCAP [7], which implements the IEC 60287 standard and the CIGRE TB 880 guidelines. This comparison is performed in terms of ampacity as well as thermal resistance estimations, showcasing the inadequacies of the IEC 60287 method.

¹ COMSOL Multiphysics® is a registered trademark of COMSOL Inc., Stockholm, Sweden.

Case Studies

In this study, submarine as well as underground cable designs are examined. The 2D geometries of these cables are illustrated in Fig. 1. The submarine cable is a typical 3C SL-type export design with a mild steel armor. As depicted in Fig. 1(a), the armor is represented as an equivalent tube with an assigned weighted thermal resistivity, effectively accounting for the presence of armor wires and bitumen within the annulus. This simplification allows for a less intricate armor depiction, resulting in a reduced number of mesh elements within the armor domain of the FEM model. Additionally, the investigation includes three single-core (1C) underground cables arranged in a spaced flat formation. Each of these cables features a smooth welded aluminum sheath, as shown in Fig. 1(b).

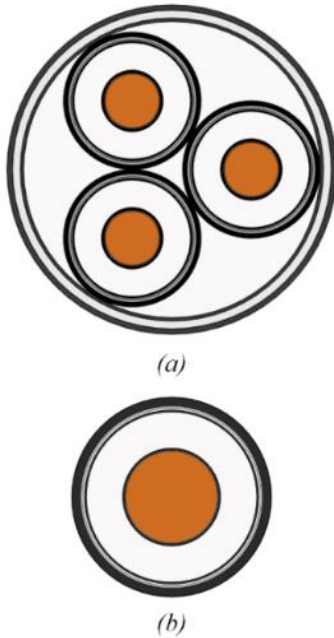


Fig. 1. 2D geometries of (a) the 3C SL-type export cable and (b) the 1C underground cable.

Both examined cases are assessed in directly buried installations. The operating and installation conditions are tabulated in Table 1.

Model Implementation

General description

Considering that the examined cables are installed directly in buried conditions with soil or seabed as the surrounding medium, the primary heat transfer mechanism is conduction. To describe this phenomenon, the developed FEM thermal model utilizes the Heat Transfer Module, specifically employing the Heat Transfer in Solids physics. The losses occurring in the dielectric and the metallic components of the cables, including conductors, sheaths, and, in the case of submarine cables, the armor, are accounted for by assigning appropriate Heat Source nodes to these specific domains.

Table 1. Operating and installation conditions.

	Submarine	Underground
Voltage [kV]	275	150
Frequency [Hz]	50	50
Bonding scheme	Solid	Single point
Burial depth (center of cable) [m]	2	3
Surrounding medium resistivity [Km/W]	0.7 (Seabed)	1.2 (Soil)
Ambient temperature [°C]	15	30
Spacing [m]	-	0.5

The applied boundary conditions (BCs) of the model are depicted in Fig. 2 for the submarine cable configuration. As it can be seen, an isothermal BC, representing the ambient temperature, is imposed on the seabed surface (or soil surface in the case of underground cables). Infinite domains are introduced on the remaining sides of the model, serving as virtual layers that extend the solution mathematically towards infinity, where thermal insulation BCs are applied [1].

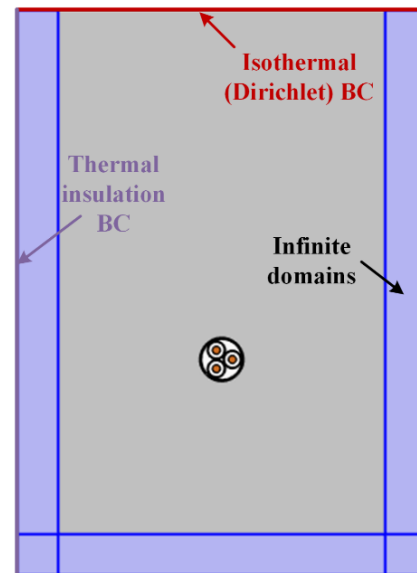


Fig. 2. Boundary conditions of the 2D FEM models.

Direct ampacity method

As previously noted, two distinct approaches are employed for the calculation of the cable ampacity. In the case of the direct ampacity method, a Dirichlet BC is imposed on the outer surface of the conductors, as illustrated in Fig. 3 for the submarine

cable configuration, with the temperature, T_{cond} , set to the thermal limit, i.e., 90°C. It is noted that the conductor temperatures of a 3C cable will be, in principle, slightly different one another. However, these differences are expected to have minimal impact on the final ampacity results. By utilizing an integration operator applied to the same surfaces, the conductor losses, denoted as W_c and measured in W/m², can be computed as follows

$$W_c = \frac{|intop1(ht.ntflux)|}{3\pi r_c^2} \quad (1)$$

where *intop1* is the integration operator, *ht.ntflux* the built-in variable for the calculation of the normal total heat flux and r_c the conductor radius. Based on the above, the cable ampacity, I_{ac} , can be determined using the following equation

$$I_{ac} = \sqrt{\frac{W_c \pi r_c^2}{R_{ac}}} \quad (2)$$

subject to

$$R_{ac} = R_{dc}(1 + y_s + y_p) \quad (3)$$

$$R_{dc} = R_{dc,@20^\circ C}(1 + a_{20^\circ C}(T_{cond} - 20)) \quad (4)$$

where T_{cond} is set at 90°C, R_{ac} is the conductor ac resistance at 90°C, R_{dc} the conductor dc resistance at 90°C, y_s and y_p the skin and proximity effect factor respectively, $R_{dc,@20^\circ C}$ the conductor dc resistance at 20°C and $a_{20^\circ C}$ the temperature coefficient at 20°C. It is worth noting that the magnetic impact of the armor wires on R_{ac} is not accounted for in (3), as the inclusion of the proposed factor 1.5 by [2] is a rather conservative approach [8].

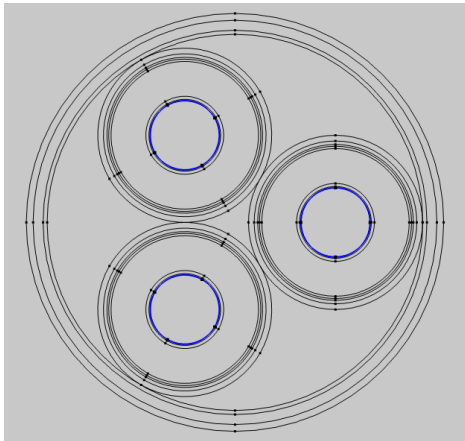


Fig. 3. Applied Dirichlet BC on the conductors' outer surface in the direct ampacity method.

In the case of the underground installation, the applied Dirichlet BC of 90°C is applied only to the middle cable, due to the observation that it experiences the hottest temperature, in the examined configuration with single point bonding. As a result, the ampacity is derived in a similar fashion as in the submarine case, but only from the losses of the middle cable.

Optimization-based method

To validate the direct ampacity method, a model that utilizes the Optimization Module is also implemented. This analysis is formulated as a least-squares optimization problem, where the attainment of the maximum permissible temperature of 90°C is set as the objective and the conductor current excitation as the control variable. The optimization problem is solved using the MMA method [9].

Numerical Results

In this section, the performance of the proposed model using the direct ampacity method is demonstrated for the aforementioned case studies. The results are compared with those obtained from both the optimization-based method and CYMCAP, which adheres to the IEC 60287 standard and the CIGRE TB 880 guidelines.

Submarine cable

For the submarine cable, the calculated ampacities using the three examined methods are tabulated in Table 2. It is evident that the two FEM-based methods yield identical ampacity values, thereby validating the accuracy of the direct ampacity method. However, the ampacity calculated based on the IEC standard exhibits a relative deviation of 2.6%.

Table 2: Ampacity comparison for the examined methods in the submarine cable case.

Method	Ampacity (A)
Direct ampacity	936.5
Optimization-based	936.5
IEC 60287 standard (+CIGRE TB 880)	961.2

This discrepancy can be explained by examining the respective thermal resistances $T_1 - T_4$ of each method, where T_1 represents the thermal resistance between the conductor and sheath, T_2 the thermal resistance of the fillers and bedding between the sheath and armor, T_3 the thermal resistance of the serving and T_4 the thermal resistance between the cable surface and the surrounding medium [2], [5]. In the FEM models, these resistances are calculated based on the following equation

$$T_{i,FEM} = \frac{\theta_{i,inner} - \theta_{i,outer}}{W_i} \quad (5)$$

where $\theta_{i,inner}$ and $\theta_{i,outer}$ are the average temperatures along the inner and outer circumferences of the examined non-metallic part i , and W_i the losses generated from the innermost metallic layer (i.e., conductors) up to the outer layer included in i . It should be noted that for T_4 , $\theta_{4,outer}$ is set equal to the ambient temperature.

The calculated thermal resistances are presented in Table 3. As anticipated from the ampacity result, the thermal resistances of the two FEM-based methods are identical and provided in the indicated "FEM" column of the table. While the FEM and IEC results exhibit excellent agreement in terms of T_1 , T_3 and T_4 , a notable relative deviation of -36% is observed in T_2 , providing a justification for the discrepancy in the estimated ampacity. This inadequacy of the IEC 60287 standard can be attributed to its assumption of isothermal sheaths, which is not applicable to 3C SL-type cables, along with the limitations of the considered geometric factor, which are discussed in detail in [3], [5].

Table 3: Comparison of thermal resistances for the submarine cable.

Thermal resistance (Km/W)	FEM	IEC 60287 standard
T_1	0.5152	0.5152
T_2	0.1413	0.0905
T_3	0.0315	0.0315
T_4	0.377	0.377

1C cables in flat formation

In the case of the three 1C underground cables in flat formation, Table 4 displays the calculated ampacities obtained through the three examined methods. Notably, an excellent agreement can be observed not only between the FEM-based methods, but also with the IEC standard.

Table 4: Ampacity comparison for the examined methods in the underground cable case.

Method	Ampacity (A)
Direct ampacity	859.3
Optimization-based	859.3
IEC 60287 standard (+CIGRE TB 880)	859.4

The computed thermal resistances T_1 , T_3 and T_4 are detailed in Table 5, confirming a good agreement, as anticipated. It should be noted that T_4 in the FEM

models in this case is not calculated using (5), but is based on the method proposed in [10].

Table 5: Comparison of thermal resistances for the underground cables.

Thermal resistance (Km/W)		FEM		IEC 60287 standard	
T_1		0.403		0.403	
T_3		0.0515		0.0515	
T_4 - Middle cable	T_4 - Outer cables	1.878	1.751	1.882	1.752

Computational considerations

The simulations are conducted on a workstation equipped with two processors Intel® Xeon® Gold 6238R and 256 GB of RAM memory.

The corresponding execution times are displayed in Table 6. Both FEM-based methods can be deemed computationally efficient in all the examined cases.

Table 6: Execution times for each FEM-based method.

Method	Submarine - Execution time	Underground - Execution time
Direct ampacity	9 s	13 s
Optimization-based	16 s	23 s
CYMCAP	3 s	3 s

Conclusions

Ampacity FEM models using COMSOL Multiphysics® software are developed and presented in this paper. COMSOL optimization module is used to verify simpler and quicker methods, such as the direct ampacity calculation, suggested in this paper. The comparison against commercial software implementing the IEC Standard method demonstrates that the developed models are not only more accurate, but also equally efficient, at least in terms of execution time. Taking accuracy together with efficiency allows for a quick design optimization, which can lead to more reliable and cost-effective cable solutions.

References

- [1] A. I. Chrysochos et al., "Rigorous calculation of external thermal resistance in non-uniform soils," in *CIGRE*, France, 2020.
- [2] Standard 60287-1-1 IEC. "Electric cables - Calculation of the current rating - Part 1-1: Current rating equations (100 % load factor)

- and calculation of losses - General”, IEC, 2014, pages 1-136.
- [3] D. Chatzipetros and A. J. Pilgrim, "Review of the Accuracy of Single Core Equivalent Thermal Model for Offshore Wind Farm Cables," *IEEE Transactions on Power Delivery*, Vols. 33, no. 4, pp. 1913-1921, Aug. 2018.
 - [4] COMSOL Multiphysics® v.6.1. www.comsol.com. COMSOL AB, Stockholm, Sweden.
 - [5] CIGRE Technical Brochure 880, "Power cable rating examples for calculation tool verification", CIGRE, 2022, pages 1-331.
 - [6] T. A. Papadopoulos, A. I. Chrysochos and M. Fotos, "Comparison of Power Cables Current Rating Calculation Methods.," in *Proceedings of the 58th UPEC 202*, Dublin, Ireland, August 29 – September 1, 2023.
 - [7] CYMCAP v.8.0 rev.02. www.cyme.com. EATON, Québec, Canada.
 - [8] CIGRE Technical Brochure 908, "Losses in Armoured Three Core", CIGRE, 2023, pages 1-159.
 - [9] K. Svanberg, "MMA and GCMMA – Fortran versions March 2013," KTH, Royal Institute of Technology, Stockholm, 2013.
 - [10] A. I. Chrysochos et al., "Determination of soil thermal resistance: A holistic approach," in *CIGRE*, France, 2022.